This study develops global estimates of ozone production and its sensitivities using satellite observations from OMI and TROPOMI. The method is complicated, which involves box model, CTMs, observations from several field campaigns, synthetic data, satellite data etc. The authors provide a fairly detailed description of the methods, but it remains unclear how these new ozone production estimates advance our understanding of ozone chemistry. My detailed comments are provided below.

We thank the reviewer for his/her constructive comments, our response follows.

1. *Title: The title begins with 'Beyond HCHO/NO2', which is confusing. What does the term 'Beyond' mean here? How is your study relevant to HCHO/NO2 From the title, one would expect that satellite HCHO/NO2 ratios are central to the analysis, but that does not appear to be the case after reading the manuscript. I'd recommend remove 'Beyond HCHO/NO2'. A novelty of this study (comparing with Souri 2025) is the use of neural network model, and it should be emphasized in the title.*

Response

We understand that readers may find it difficult to see the connection between FNR and the present study at first sight. To address this ambiguity, we need to provide clearer context and revise the title accordingly.

As stated in the introduction, our work aims to provide two key outputs:

1. **The magnitude of net PO3: essential for identifying where ozone is locally produced or lost through secondary chemical pathways.**
2. **Sensitivity maps of PO3 to local NO2 (a proxy for reactive nitrogen) and HCHO (a proxy for VOC reactivity), which are critical for guiding emission control strategies.**

Traditional data-driven approaches that use satellite observations to diagnose ozone sensitivities to VOCs and NOx have primarily relied on FNR-based segregation of NOx-sensitive, transitional, and VOC-sensitive regimes. These thresholds are derived from various model realizations, and their error structures have been characterized in Souri et al., 2023 and the references therein: https://acp.copernicus.org/articles/23/1963/2023/

However, FNR has major blind spots:

1. **Lack of sensitivity magnitudes: FNR only classifies regimes without quantifying the actual magnitude of ozone sensitivities. For example, if $\partial P_{O_3}/\partial NO_2$ is +10 s^{-1} or +3 s^{-1}, both would be labeled "NOx-sensitive," even though their regulatory implications might be different. What truly matters about emission control is the magnitude of these responses. For this reason, CTM-based calculations (either through direct decoupled methods, perturbation or adjoint approaches) are typically used. These, however, require extensive efforts to constrain model inputs with satellite data (see Souri et al., 2020: https://acp.copernicus.org/articles/20/9837/2020/).**

Our work provides quantitative first-order sensitivity maps, equivalent to directional derivatives (Appendix A), which is a major innovation of the new algorithm.

2. **Lack of adequate dimensions: FNR slices the inherently multidimensional, nonlinear system into just two dimensions. To demonstrate this shortcoming, we perturbed photolysis rates over polluted regions during the KORUS-AQ campaign using observationally-constrained F0AM model. Multiplying photolysis rates by factors of 0.5 (dim, left), 1.0 (default, middle), and 2.0 (bright, right) produced three sets of PO3 isopleths.**

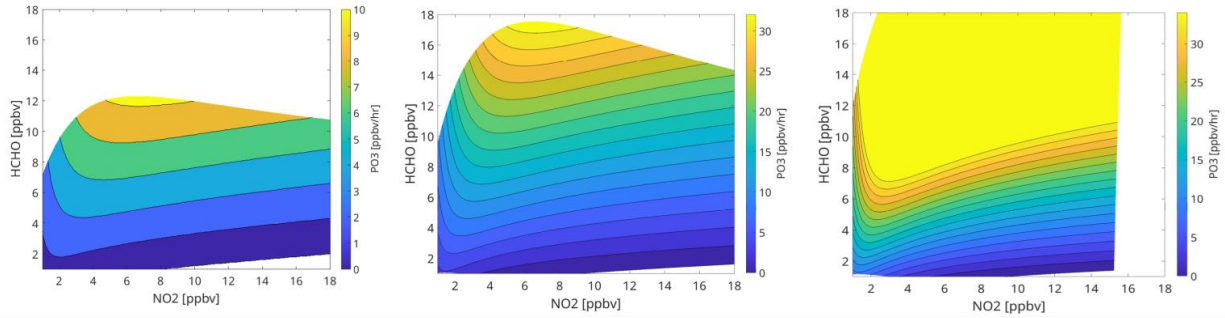

The results clearly show that increasing light intensity raises both net PO3 and its sensitivities to NOx and VOC (the contours are more compact in the bright case; each contour corresponds to 3 ppbv/hr). This means that the same FNR can correspond to entirely different magnitude of sensitivities depending on available light. Although one might expect FNR to indirectly reflect variations in photolysis rates, our analysis of 47,000 data points obtained from KORUS-AQ measurements showed no relationship between measured jNO_2 and FNR:

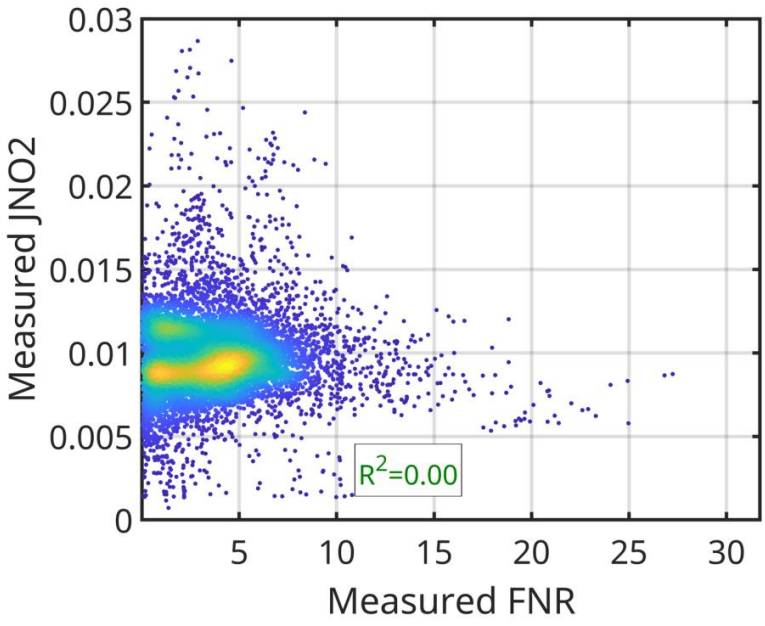

A similar limitation arises from FNR's inability to account for water vapor effects on PO3. Capturing these complex nonlinear interactions between PO3, light, humidity, and precursor concentrations requires more advanced methods over a simple ratio, lacking any information about light intensity and humidity. In a data-driven framework, this is best achieved using nonlinear parameterizations such as DNNs.

This new product therefore represents a paradigm shift away from oversimplified FNR approaches. It not only provides spatiotemporal sensitivity magnitudes, but also accounts for multidimensional dependencies. We highlight this feature in Section 4.3.

For these reasons, we strongly believe this message deserves to be reflected in the title of the paper: it signals a shift toward a more rigorous, multidimensional exploitation of satellite observations for ozone chemistry.

Modifications

To better inform how the new sensitivity maps can eliminate the need for FNR and to highlight the machine learning aspect, we added:

"Beyond Binary Maps from HCHO/NO_2: A Deep Neural Network Approach to Global Daily Mapping of Net Ozone Production Rates and Sensitivities Constrained by Satellite Observations (2005–2023)"

While we had provided context about the advances made compared to FNR, we added a paragraph in the introduction describing why we should quantify the multidimensional magnitude of PO3 sensitivity, currently lacking in FNR-based approaches. We added in the introduction:

The overarching goal of producing ozone chemistry sensitivity maps is to inform regulatory agencies about the impact of emission reductions on locally produced ozone. Unlike conventional FNR-based binary maps, these maps must quantify the magnitude of sensitivity rather than merely indicating its direction. This quantitative approach is essential because both the sign and magnitude of sensitivities are crucial for understanding the impact of emission changes. While detailed sensitivity maps can be derived from chemical transport models by perturbing underlying emissions, the lack of observational constraints on these models can introduce significant biases. Souri et al. (2025) attempted to address this limitation by providing magnitude-dependent sensitivity maps of PO_3 to NO_2 and HCHO using piecewise linear regression. However, their approach yielded derivatives of PO_3 with respect to NO_2 and HCHO that remained invariant with changes in light and humidity conditions. This limitation is problematic because reduced light conditions are known to substantially dampen the sensitivity of PO_3 to NO_x and VOCs, even under identical emission rates. The current work is therefore motivated by the need to capture the complex, multidimensional dependencies of PO_3 on ozone precursors, light intensity, and humidity using a more flexible data-driven approach through a machine learning algorithm. While these maps will not replace process-based chemical transport model experiments, they can efficiently provide first-order assessments to: (i) strategize top-down modeling experiments, (ii) gauge the added value of satellites on predictions of PO_3, and (iii) guide the design of sub-orbital missions in regions with poorly documented elevated PO_3.

2. *For the abstract, the opening should clearly define the scientific question being addressed, rather than starting with the discussion of the FNR, which is not the main focus of this study. My understanding is that this work aims to derive PO3 from a DNN model, which is different from the indicator ratio or FNR approach. The repeated references to FNR throughout the abstract are confusing and should be reconsidered.*

Response

Our work aims to generate two key products: the net PO3 and the magnitude of PO3 sensitivities to NO2 and HCHO. These two pieces of information are essential for identifying ozone production hotspots and assessing their sensitivity to local pollution levels. This central message should be highlighted in the abstract.

Over the past two decades, we have extensively explored the application of FNR in diagnosing ozone chemistry (e.g., Duncan et al., 2010; Souri et al., 2020; Souri et al., 2023). While FNR has been a valuable first step in demonstrating the utility of satellite observations to classify ozone chemical regimes, it ultimately offers only a binary perspective on a fundamentally continuous and multidimensional problem. Therefore, it is essential to highlight this new fresh paradigm.

Modifications

In the supplementary, we added a new section describing the fundamental issues with FNR; we did not include it in the main draft because it is more of a reminder for people who may misuse FNR rather than bringing new insights into ozone chemistry.

1. FNR is oblivious to the impact of photolysis rates and water vapor content on PO_3

The primary objective of using the formaldehyde-to-nitrogen dioxide ratio (FNR) is to reduce high-dimensional, non-linear ozone production rates into a two-dimensional framework based on volatile organic compound reactivity (VOCR) and reactive nitrogen. However, beyond the fact that HCHO and NO_2 does not fully represent VOCR and reactive nitrogen, it is crucial to recognize that ozone production rate sensitivities and magnitudes depend on other geophysical variables independent of FNR. Among these variables, photolysis rates and water vapor are major drivers of atmospheric oxidation capacity, modulating numerous reactions related to ozone production (Kleinman et al., 2001).

To demonstrate photolysis rate effects on both PO_3 magnitudes and sensitivities, we conducted F0AM box model simulations constrained by geophysical variables during June 6-9 of the KORUS-AQ campaign (Souri et al., 2025). We perturbed NOx, VOCs, and photolysis rates to generate three sets of isopleths (Figure S1). The results clearly show larger ozone production rates under more intense light conditions. More importantly, the contours corresponding to identical PO_3 intervals (3 ppbv/hr) become more compact under brighter conditions, indicating that PO_3 becomes more sensitive to both NO_X and VOCs with increased light intensity. This pattern suggests that identical FNR values under different photolysis rates can have fundamentally different implications for ozone production rate sensitivities.

To confirm that FNR contains no photolysis rate information, we analyze paired FNR and jNO_2 photolysis rate measurements from over 47,000 data points during the KORUS-AQ campaign, revealing no correlation between these variables (Figure S2). This demonstrates the need for additional dimensions in ozone sensitivity analysis, necessitating more sophisticated algorithms (like our approach) over traditional threshold-based methods.

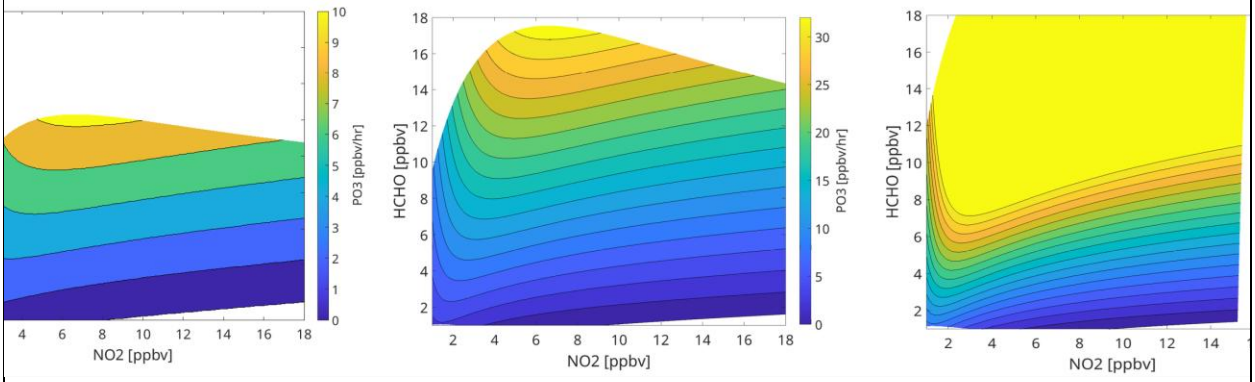

Figure S1. The PO_3 isopleths generated using F0AM box models derived from observations taken during the KORUS-AQ campaign under three different photolysis rates scenarios: (left) multiplied by 0.5, (middle) default, (right) multiplied by 2.0. Each contour represents 3 ppbv/hr.

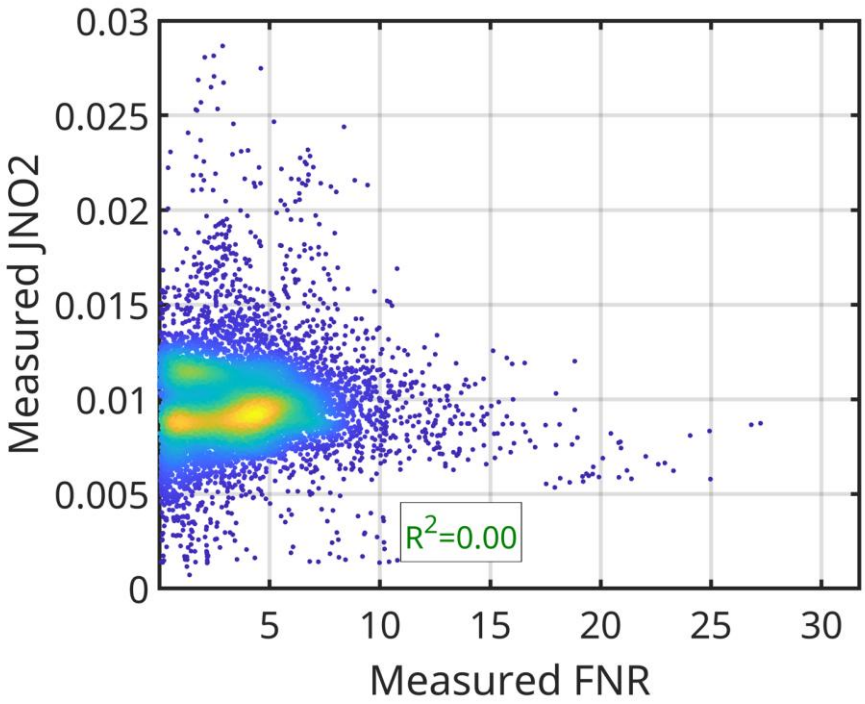

Figure S2. The comparison of measured FNR and measured jNO_2 frequencies taken from aircraft observations during the KORUS-AQ campaigns. All measured points are used to make this plot.

Figure S3 illustrates the representation of ozone sensitivities by mapping five variables derived from TROPOMI and our PO_3DNN parameterization across two seasons over Los Angeles.

FNR values are low during colder months due to abundant NO_2 relative to HCHO, qualitatively suggesting the LA region should be predominantly VOC-sensitive. However, the derivatives and sensitivities of PO_3 to both HCHO and NO_2 remain muted due to limited photochemical activity, making PO_3 unresponsive to NO_X and VOC concentrations. Conversely, summer conditions yield larger derivatives, showing much stronger PO_3 responses to both species. This example can be extended to different times of day, such as FNR values from geostationary satellites or morning versus afternoon measurements from low Earth orbit satellites.

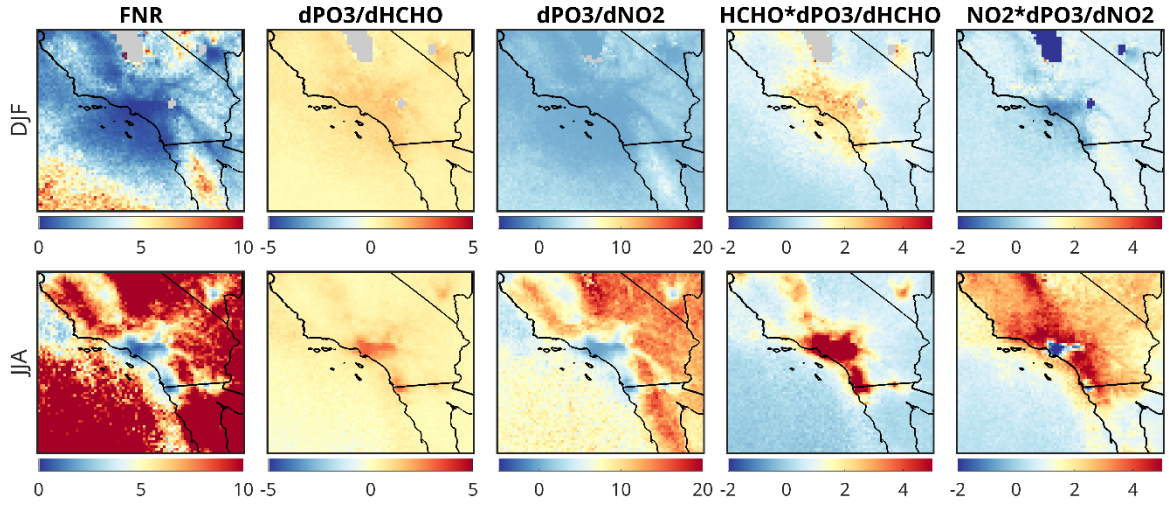

Figure S3. Five variables derived from our PO_3DNN product based on TROPOMI dataset. The first row focuses on December-January-February (DJF), while the second row shows those variables for June-July-August 2023. The calculation of the sensitivities and derivatives are based on perturbation of the DNN algorithm described in the main paper.

The absence of PO_3-relevant geophysical information in FNR also applies to water vapor. F0AM box simulations over polluted regions show that increasing humidity enhances PO_3 through the generation of two OH molecules via H_2O+O^1D reactions (Figure S4). However, FNR contains no water vapor information, as humidity is driven by hydrological and meteorological factors decoupled from the processes determining FNR (Figure S5). This further necessitates adding water vapor as an additional dimension in ozone sensitivity

analysis.

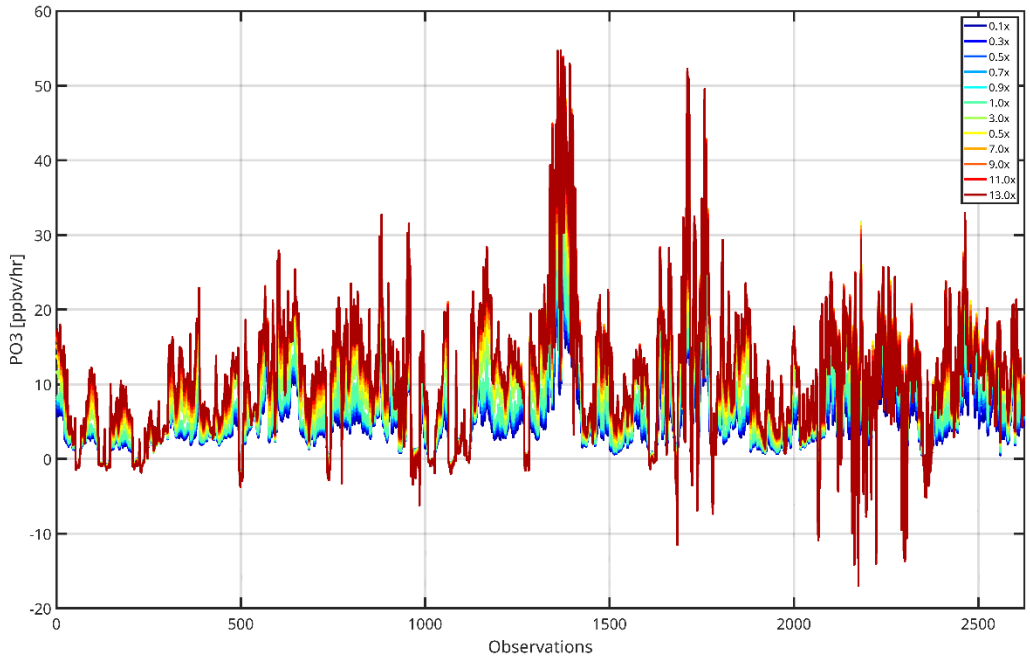

Figure S4. The effect of $H_2O(v)$ on PO_3 during KORUS-AQ campaigns. Only highly polluted regions ($HCHO \times NO_2 > 10$) are selected for this experiment.

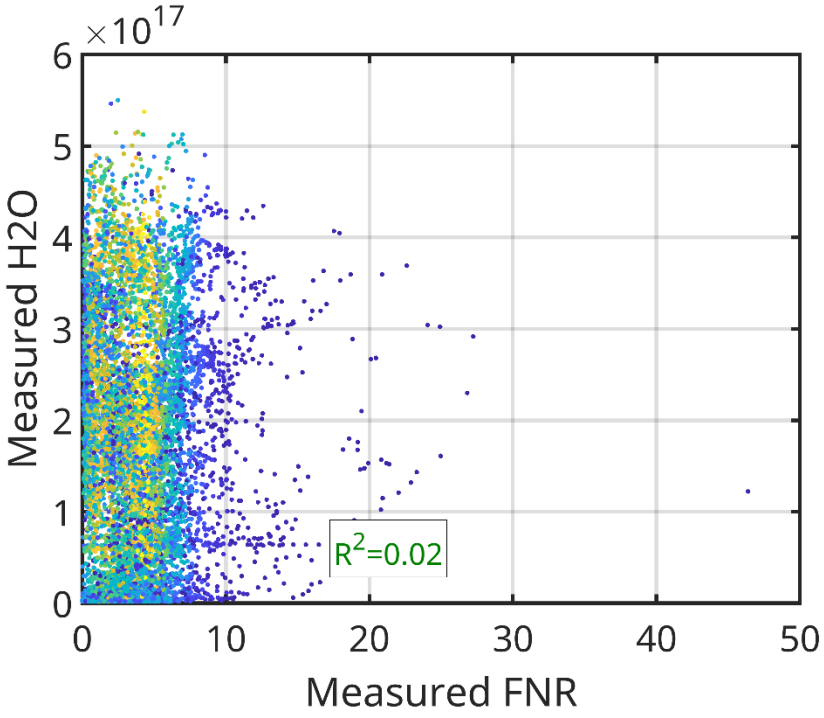

Figure S5. The comparison of measured FNR and measured water vapor density taken from aircraft observations during the KORUS-AQ campaigns. All measured points are used to make this plot.

3. *This study appears to be a follow-up study of Souri et al. 2025 with some technical improvements, such as use of DNN. While the technical enhancements are clear, the added scientific value is not. It is unclear how the improved PO3 estimates advance our understanding of ozone formation processes. Many figures, including the spatial maps and seasonal variations, are quite similar to those presented in Souri et al. (2025). The main difference seems to be the extension of the study period from one year to multiple years (2005–2023), but only two regional case studies are analyzed for long-term trends. I suggest expanding the long-term trend analysis globally to better demonstrate the added value of this extended dataset.*

Response

Thanks for the suggestion about expanding the trend analysis globally. While we recognize that our previous work has similarities with respect to PO3 predictions compared to the current work, there are distinct differences which are documented in in the paper (improved prediction, more cohesive between remote and polluted regions, substantially reduced noise, and less discretization). In fact, it is encouraging to see that both algorithms provided consistent results on average. The most innovative part of the current approach lies in its ability to provide a more comprehensive sensitivity maps compared to Souri et al., 2025.

We decided to add a global trend analysis (2005-2019) of PO3 with respect to NO2 and HCHO using OMI in the manuscript. We do not intend to include TROPOMI in the long-term analysis because it will require a data harmonization approach which is still under investigation within our team (the objective of the third year of our ACMAP-Aura project). In addition, the long-term stability of OMI radiance has made it a great product to study trend.

Modifications

We moved the trend analysis of Tehran and LA to the supplementary material, and replaced that with a global analysis.

We added these global findings to the abstract, introduction and conclusion.
In the abstract:

The stability and long-term records of OMI retrievals (2005-2019) enable us to provide the first global maps of PO_3 linear trends showing a surge of >20% over China, the Middle East, and India, while a reduction in the eastern U.S., southern Europe, and several regions in Africa.

In the conclusion:

The long record of stable observations from OMI allowed us to generate the first-ever maps of PO_3 linear trends from 2005 to 2019 globally. The global long-term trends revealed substantial spatial variability, with predominantly positive trends over Asia and the Middle East (>30% relative to 2005 in some regions) and negative trends across the eastern U.S., Europe, and parts of Africa. Analysis indicated that simultaneous changes in HCHO and NO_2 boundary layer concentrations were the primary drivers of these trends. Although increases in both precursors over Asia and the Middle East, rising PO_3 and reduced concentrations elsewhere lead to decreases, localized non-linearities complicated this relationship, as demonstrated by contrasting chemical regimes in Tehran vs. Los Angeles. Quantitative attribution of these trends presents significant challenges because of their small amplitudes relative to seasonal variations and non-linear sensitivities in the parameterization, necessitating "hold-one-out" approaches that account for complex interdependencies between input variables.

4.4.3. Global PO_3 linear trends using OMI (2005-2019)

Using the linear trend calculation method outlined by Souri et al. (2024), we compute global long-term linear trends of PO_3 from OMI data, shown in Figure 8. High-latitude regions (>65°) are excluded due to limited photochemical activity. We observe large variability in both the signs and magnitudes of the linear trends. Predominantly positive trends occur over the Middle East, India, and China, while negative trends are mostly found in the eastern U.S., maritime Southeast Asia, and several areas in Africa. The largest upward trend in PO_3 over the U.S. occurs in oil and gas producing regions, including the Permian Basin. While various physicochemical processes beyond near-surface PO_3 influence tropospheric ozone trends, the strong agreement between predominantly upward PO_3 trends in Asia and the Middle East and satellite-based ozone observations (Gaudel et al., 2018; Boynar et al., 2025) is noteworthy.

To gather a more relative perspective, Figure 9 shows relative PO_3 trends (as percentages relative to 2005 annual averages) for regions where PO_3 exceeds 0.5 ppbv/hr. The largest relative changes (>30%) are evident over the Persian Gulf, Chile, India, and China. Large negative values dominate over the eastern U.S. and over the central Africa (>20%).

Multiple factors in our parameterization can simultaneously influence these trends, including changes in HCHO VCDs, NO_2 VCDs, dynamic changes in column-to-PBL conversion factors from MINDS, water vapor, and photolysis rates. However, photolysis rate trends should be negligible because long-term changes in total overhead ozone are insignificant at midlatitudes (Souri et al., 2024), and surface albedo is based on a monthly climatology dataset. While water vapor increases over time in response to global warming (Souri et al., 2024; Borger et al., 2024), these changes are insufficient to explain the large variability in PO_3 linear trends over polluted regions. Accordingly, simultaneous changes in HCHO and NO_2 boundary layer mixing ratios are the main drivers of PO_3 trends.

The PO_3 trends are generally explained by changes in ozone precursor concentrations which are mapped in Figures S10 and S11. The attribution of trends in OMI HCHO and NO_2 have been partly discussed in Souri et al., 2024 and the references therein. Increases in both HCHO and NO_2 over the Middle East, India, and China drive rising PO_3 over time. Conversely, reduced HCHO and NO_2 concentrations over parts of Africa, the eastern U.S., and maritime Southeast Asia, have led to PO_3 reductions. However, many localized areas exhibit strong non-linearity. For instance, Tehran (Iran) shows positive PO_3 trends (Figure S13) caused by NO_2 increases in a predominantly VOC-sensitive regime, reducing ozone loss through NO_2+OH

reactions. Los Angeles (USA) shows upward trends attributed to rapid NO_2 reductions, resulting in the opposite effect (Figure S14).

The quantitative characterization of these trends (similar to our analysis of PO_3 seasonality in Section 4.4.2 or rapid PO3 changes during a heatwave in Text S2) presents significant challenges for several reasons: (i) the amplitudes of these trends are generally an order of magnitude smaller than seasonal changes, requiring more stringent attribution methods, (ii) the sensitivities of PO_3 to input parameterization can behave non-linearly, making a linear trend analysis ill-suited for some localized areas, and (iii) changes in ozone precursors have effects on the sensitivity of PO_3 to photolysis rates as described in Section 4.4.2, introducing a convoluted problem.

Since our PO_3 parameterization encapsulates non-linear and interdependent relationships between pollution levels, light intensity, and water vapor, fully isolating individual effects on PO_3 trends requires reproducing the product while holding either NO_2 or HCHO constant individually and allowing others to evolve over time (an approach similar to modeling experiments in Souri et al., 2024). This approach comprehensively captures the non-linear dependencies between input variables and PO_3, circumventing the need for crude linear approximations.

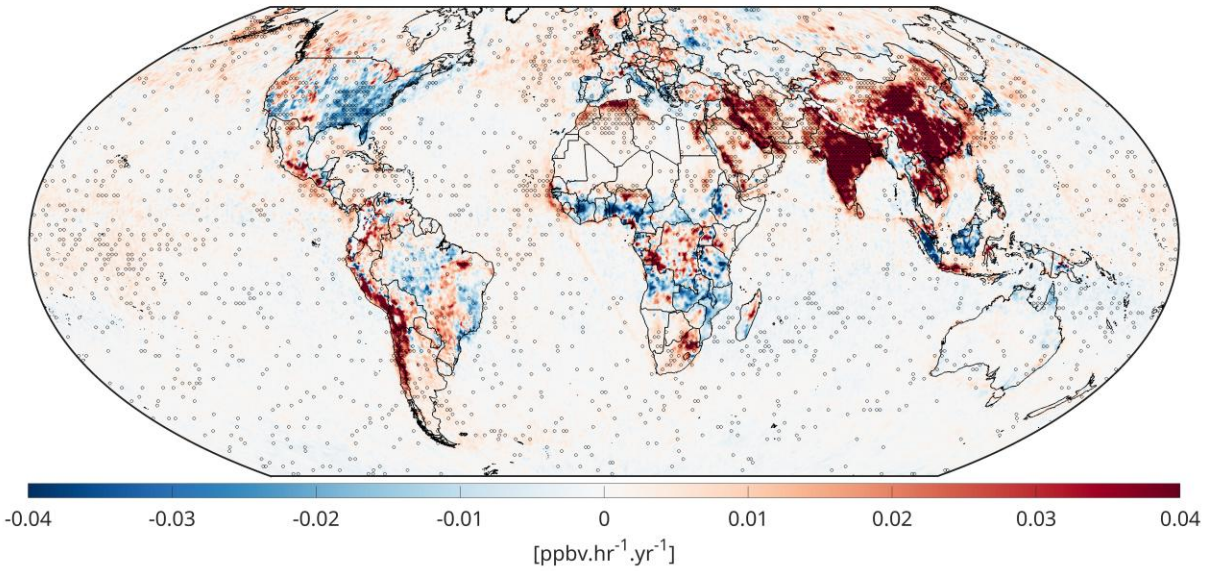

Figure 8. The linear trend maps of PO_3 within PBL derived from our new algorithm using OMI in 2005-2019. Dots indicate that the trend has passed the Mann–Kendall test at 95% confidence interval.

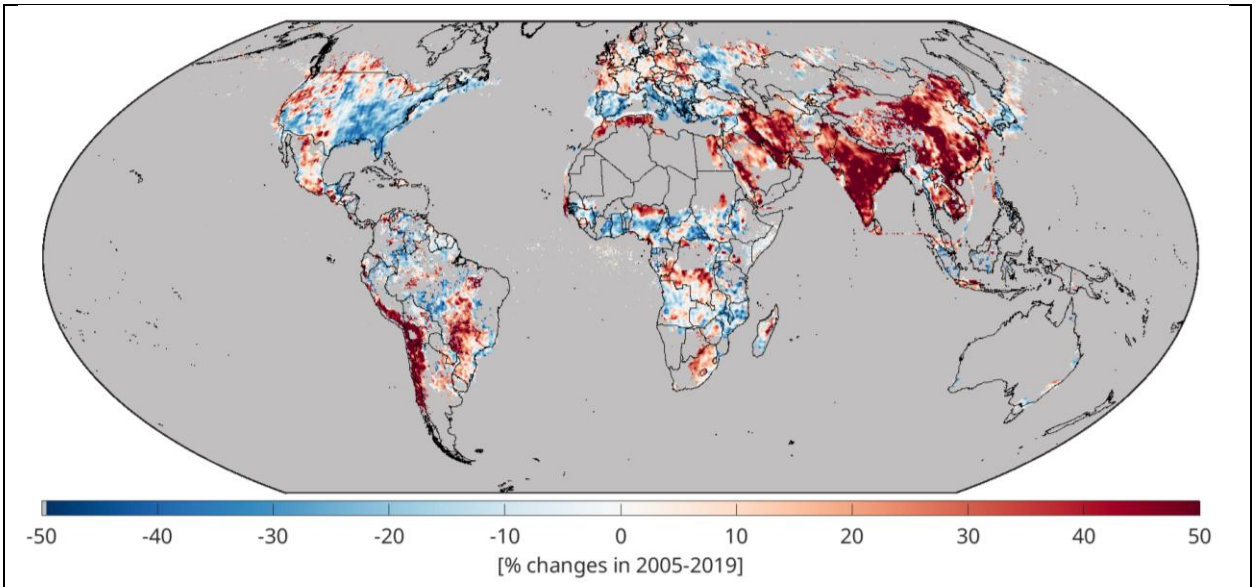

Figure 9. Similar to Figure 8 but percentage changes are instead shown over PO_3>0.5 ppbv/hr.

4. *It is unclear to me why a satellite-based PO3 product is needed. PO3 is essentially a "modeled" quantity, which is not directly observable. There is no way to evaluate the robustness of PO3 estimates. The magnitude of PO3 can vary depending on how you define the PO3, whether it's accumulative production or instantaneous production. It seems that the authors are looking into net production of O3, but it is not clear how the chemical loss of O3 is defined, and how the uncertainties of chemical loss terms would influence the magnitude of PO3.*

Response

We respectfully disagree with this comment.

PO3 is not purely a modeling quantity but is measurable using specialized dual-tube instruments (Cazorla and Brune, 2010; Sadanaga et al., 2017; Sklaveniti et al., 2018), as mentioned in our introduction. These instruments can provide valuable insights into chemistry representation in models. While measurement uncertainties are decreasing over time, these instruments remain in the development stage, and we believe our product could help accelerate their improvement and deployment.

We carefully considered how to define PO3 to enable seamless intercomparison with future PO3 estimates. Previously, we examined individual reaction rates defining both production and loss terms (e.g., Souri et al., 2020). However, explicitly defining these terms creates challenges for direct comparison across different chemical mechanisms. For instance, peroxy radicals (RO2) are defined differently among various chemical mechanisms, and some VOC and organic nitrate definitions are inconsistent (some mechanisms use lumped species while others separate them).

A practical approach for defining PO3 in this context is to calculate the instantaneous PO3 tendency by summing all chemical loss pathways of ozone (negative stoichiometric

coefficients) and all chemical production pathways (positive stoichiometric coefficients). This approach closely matches the output from chemical solvers in atmospheric models under steady-state conditions and facilitates intercomparison procedures. While we lose some chemical interpretation regarding individual chemical terms shaping PO3, our product focuses on net values rather than parameterizing individual terms.

We acknowledge that we cannot directly validate F0AM PO3 against measurements due to the absence of PO3 observations during the suborbital missions. However, PO3 is influenced by numerous geophysical variables that are either directly or indirectly constrained in our box model (Section 4.1 in https://acp.copernicus.org/articles/25/2061/2025/). Examination of individual terms defining PO3 in the CB06 mechanism shows that nearly all are well-constrained in our simulations: we accurately reproduced NO and NO2 compared to aircraft measurements, constrained many VOCs yielding reasonable HCHO simulations against observations, and reproduced HO2 and OH with minimal biases and high correspondence within instrument noise levels. The first-order approximation of PO3 in urban settings (NO+HO2 minus NO2+OH) involves species that are all well-captured in our model.
The primary uncertainty lies in RO2, which serves as a proxy, highlighting where specialized PO3 instruments could help validate constrained PO3 estimates across different chemical mechanisms and heterogeneous chemistry treatments.
While we do not claim complete alignment with actual PO3 values (which cannot be verified due to absent measurements), we believe our box model simulations provide reasonable constraints on the various terms contributing to PO3.

Modifications

We improved the wording around the PO3 definition in the methodology:

Once the simulations are done, we determine simulated PO_3 by:

$$PO_3 = FO_3 - LO_3 \quad (1)$$

where LO_3 is all possible chemical loss pathways of ozone (negative stoichiometric multiplier matrix) and FO_3 is all possible chemical pathways producing ozone molecules (positive stoichiometric multiplier matrix). This equation is also known as ozone tendency. This definition simplifies intercomparison with estimates derived from different chemical mechanisms by eliminating the requirement to explicitly match individual production and loss terms, which often exhibit inconsistencies across mechanisms, especially in their treatment of peroxy radicals. The calculation of PO_3 is under a steady-state assumption.

5. *The authors claim that photolysis rates and water vapor have large influence on PO3. However, their calculations of these quantities appear oversimplified. It is unclear how cloud and aerosol effects on photolysis are accounted for. Water vapor and total ozone columns are taken from MINDS simulations, even though satellite-based observations for*

these variables are available. It is not clear why satellite data are only used for NO2 and HCHO but not for other relevant parameters. This inconsistency needs to be addressed.

Response

No single satellite can reliably measure near-surface water vapor (H2O(v)) at the spatial coverage provided by TROPOMI and OMI. Available satellite capabilities vary significantly: some measure only total column water vapor (MODIS, OMI, TROPOMI), others provide vertical profiles with limited near-surface sensitivity (IASI, AIRS), and GPS radio occultation provides sparse but accurate profiles. The diversity of surface-based, sounding, and satellite instruments for water vapor retrieval, each with unique strengths and limitations, has motivated efforts to integrate them within harmonized frameworks through data assimilation. This approach provides optimal H2O estimates by accounting for varying vertical sensitivity, spatial representation, and sensor-specific artifacts and errors.

We leveraged the well-established MERRA-2 "replay" data assimilation framework, which constrains water vapor using numerous observational products. Our validation against SSMIS integrated water vapor (IWV) (recognized as the most robust water vapor product over oceans, which comprise 71% of Earth's surface) shows minimal biases in 2005 with replay mode enabled in a GEOS-simulation performed in Souri et al. (2024) (figure below).

Our sensitivity analysis reveals that PO3 responses to H2O variations are generally an order of magnitude smaller than those for photolysis rates (Js), NO_2, and HCHO, typically ranging around 1-2 ppbv/hr per unit of water vapor density. Therefore, having 1-5% uncertainties in simulated water vapor should not significantly impact our results and would remain even smaller than DNN estimator errors.

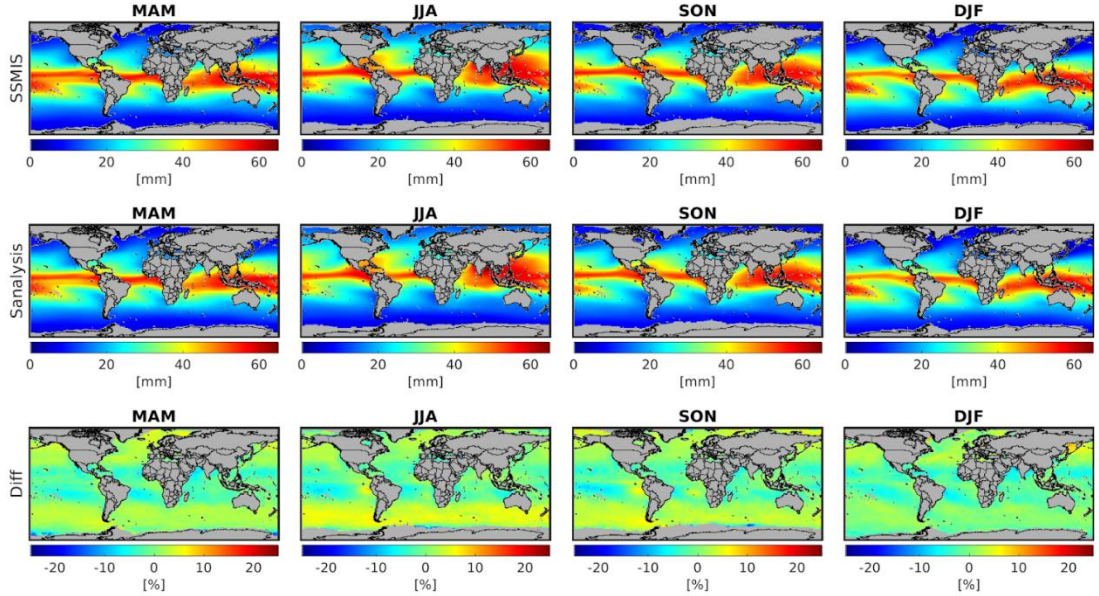

Likewise, total ozone columns are constrained by satellites in MINDS with only 2-3% error (see Figure S1 in https://acp.copernicus.org/articles/24/8677/2024/acp-24-8677-2024-supplement.pdf). Their errors can be safely ignored.

Regarding the impact of aerosols and clouds on photolysis rates, we agree that they can partly introduce biases in our estimates, as discussed in the paper. This error has been largely mitigated by removing clouds/aerosol using the effective cloud fraction being sensitive to all those particles.

There are known physical models to scale photolysis rates given the optical properties of particles (such as FAST-JX or RACM). However, it is not feasible to source 3D optical properties of aerosols and clouds at the same resolution and time as of TROPOMI and OMI globally. While some instruments like TROPOMI can provide 2D optical properties, we are required to know how much of these are below PBL and how much are above it. There are also complexities about the height of aerosols, because aerosol layer height from TROPOMI or OMI is optical centroid and not the physical top boundary. Knowing these optical properties (partial AOD, SSA, and phase functions) is essential.

Similar to the discussion about water vapor, we need a data assimilation approach to exploit various ground and space remote sensing instruments to constrain aerosols and cloud optical properties in models. But this is much more challenging compared to the water vapor problem, because aerosols and clouds are affected by a larger number of physiochemical processes. While we could have used MINDS cloud/aerosol optical properties to supposedly scale photolysis rates, we think the errors and mismatches of the model would have harmed the analysis.

We also need to emphasize that the effective cloud fraction is not equal to geometrical cloud fraction (defined in meteorology). The O2-O2 algorithm is sensitive to the amount of contamination by clouds (even over sensitive to thin clouds), making the cloud flag a effective to mask them. To show some showcases for our daily OMI PO3 product:

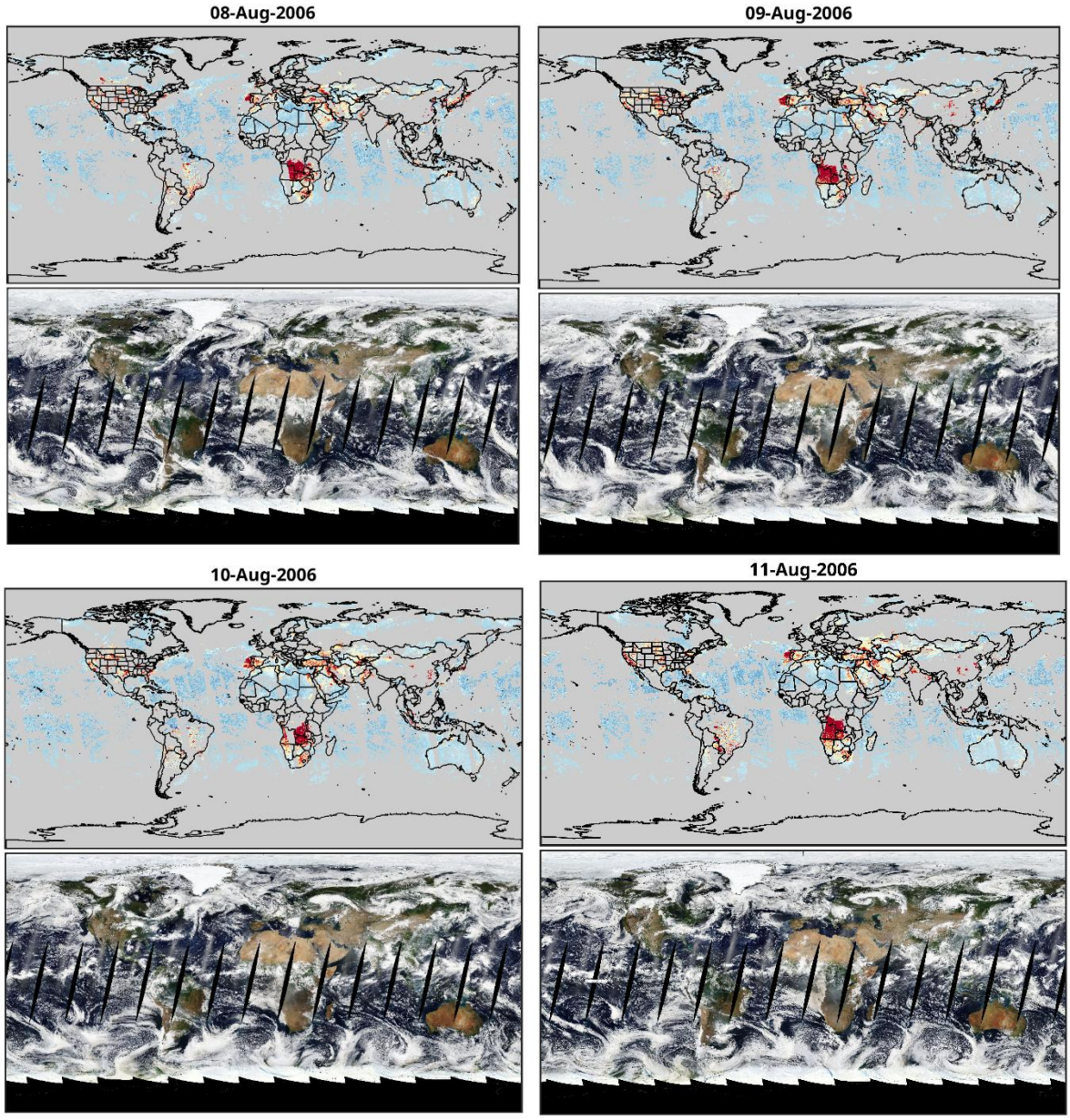

and TROPOMI:

03-Aug-2021

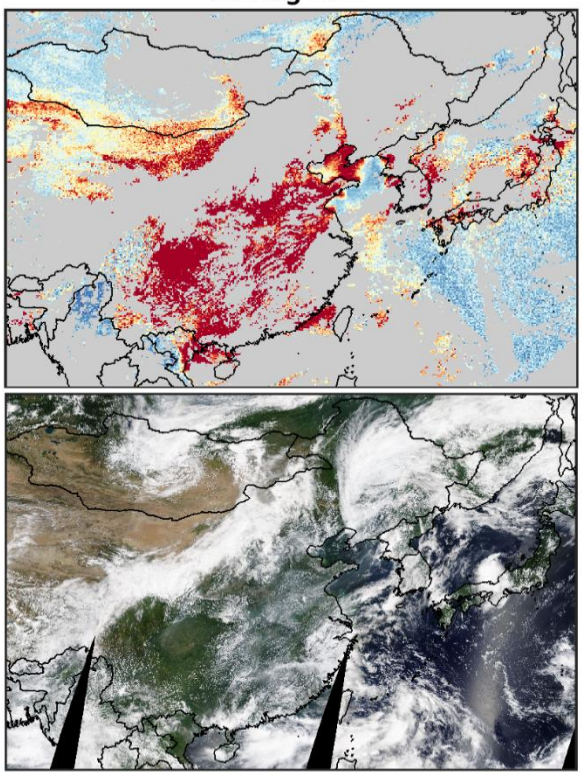

This is another TROPOMI case that shows in strong smoky areas in California, the quality flags removed most of the contaminated pixels (but not all).

09-Jun-2023

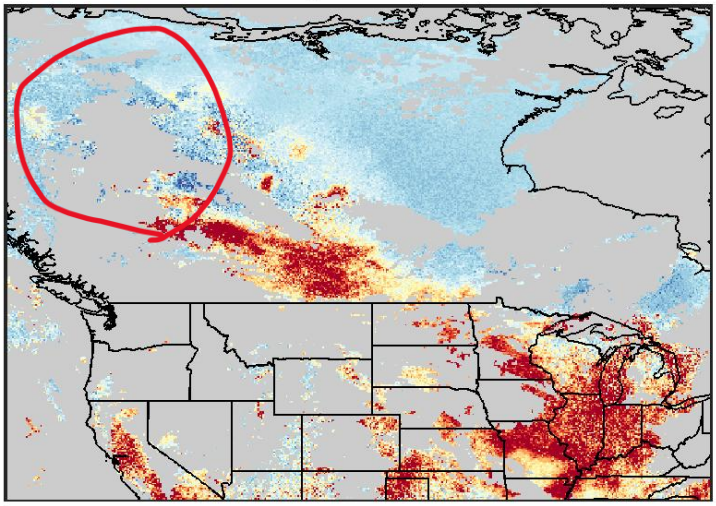

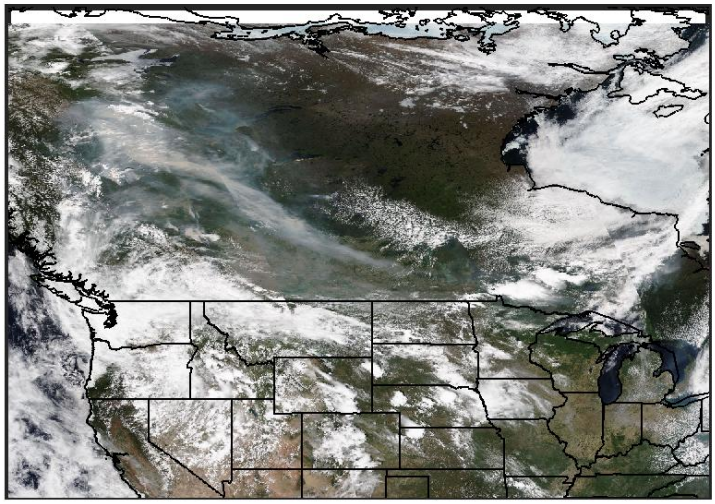

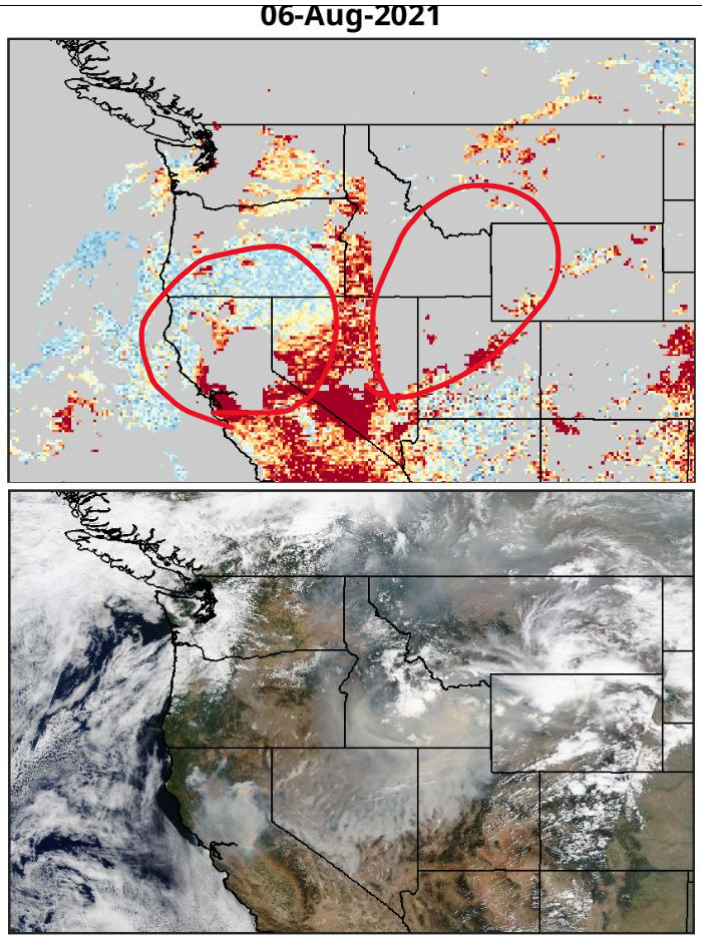

Modifications

To address this comment, we moved the discussion about the effect of clouds and aerosol in Stage 1 to the error analysis part and added more caveats:

It is important to acknowledge that the defined total error budget here is only a good guess and optimistic. Some underlying sources of error, which are difficult to quantify, are not included. For example, errors related to the training dataset derived from the F0AM model are challenging to assess because of the lack of PO_3 measurements. We assume other inputs to the PO_3 parametrization, such as the monthly climatology TROPOMI surface albedo to be error-free. Additionally, all datasets used to estimate PO_3 contain spatial representation errors (Souri et al. 2023), which are difficult to measure without knowing their true state of global spatial variability. It is worth noting that some of the inputs such as $H_2O(v)$ and the overhead ozone column have minimal biases because of MINDS simulations being observationally constrained (Fisher et al., 2024; Souri et al., 2024).

Another source of uncertainty arises from partially cloudy pixels and aerosols, which can introduce errors in calculated photolysis rates. While we successfully filtered out cloud cover and strong aerosol loadings (e.g., from wildfires) using effective cloud fraction thresholds, some aerosol or cloud-contaminated pixels may pass cloud screening due to low optical depth or height characteristics. Rigorously quantifying the errors coming from these effects would require running a radiative transfer model with detailed three-dimensional optical properties of

clouds and aerosols on a global scale, particularly critical for aerosols, which can have complex effects on photolysis rates depending on their absorption and scattering properties and vertical distribution. Unfortunately, such comprehensive datasets are typically limited to the narrow swaths of spaceborne lidar observations, which themselves carry substantial uncertainties (Thorsen and Fu, 2015). While these complications cannot be entirely avoided, particularly for aerosol effects, users can apply additional quality control measures by filtering pixels using aerosol optical depth retrievals from TROPOMI, OMI, or other sensors to more rigorously identify contaminated observations.

6. *The authors demonstrate the use of PO3 through some case studies, but these studies are somewhat disconnected. Each focuses on a different region and time period (e.g., northeastern U.S., Middle East, Los Angeles, Tehran), resulting in a fragmented narrative that feels like a collection of isolated examples. I recommend reorganizing these sections to tell a more cohesive scientific story. The analysis of long-term trends is promising. Expanding this analysis to the global scale, and examining how ozone production sensitivities have evolved over time, would substantially strengthen the manuscript.*

Response

We agree that these are different applications which were meant to provide more confidence in the utility of our product from different angles. We reordered some of the sections and moved some to the supplementary materials to have a more cohesive flow.

Modifications

We renamed Section 4.4:

PO_3 Maps and Sensitivities using OMI and TROPOMI: A General View, Long-term analysis, and Intercomparisons

Now this section starts with 4.4.1. Global PO_3 and Seasonality using OMI in 2005-2007
The reason behind it is that 2005-2007 is when OMI signal was strong and did not go through the row anomaly issues. We then have their attributions in *4.4.2. The attribution of PO3 seasonality***.**

We then introduced "4.4.3. Global PO_3 linear trends using OMI (2005-2019)**" to keep the discussion focused on OMI.**

Then we introduce TROPOMI and its intercomparison with OMI. This is good bridge to move from OMI to TROPOMI while having some joint discussion: *4.4.4. High resolution TROPOMI-based PO3 maps contrasted with OMI in 2019*

Then we have *4.4.5. Error Analysis* **to discuss both OMI and TROPOMI errors on a monthly basis.**

Finally, we have this section separating the sensitivity map analysis from the rest: 4.4.6. Beyond binary maps: Ozone sensitivity maps using high-resolution TROPOMI data

As a result, the discussion about LA and Tehran and the heatwave effect have been moved to the supplementary. We think the new layout is more cohesive than before.

7. *The DNN model is trained using F0AM-simulated data. Although the model shows reasonable performance, the derived relationships remain model-dependent and limited by the diversity of available field campaigns. Rather than randomly withholding data for testing, it would be more informative to exclude one or two entire field campaigns from training and test whether the DNN performs well out-of-sample. This approach would better demonstrate the model's robustness and generalizability.*

Response

Thanks for the suggestion! We performed the similar experiment as the reviewer suggested for PO3LASSO in Souri et al., 2025, but we decided to show "test" data as they were never used for hyperparameter tuning. We added this new figure in the supplementary with the campaign-specific withholding figure, compare to Figure 7 in Souri et al., 2025.

Modifications

We added:

Similar to the approach of Souri et al. (2025), we completely exclude each suborbital mission from the training dataset and use it as an independent benchmark to evaluate the model's performance. The resulting accuracy is comparable to that achieved when 56% of the data are used for training, indicating that the PO_3 parameterization has reached a high degree of generalization (Figure S10).

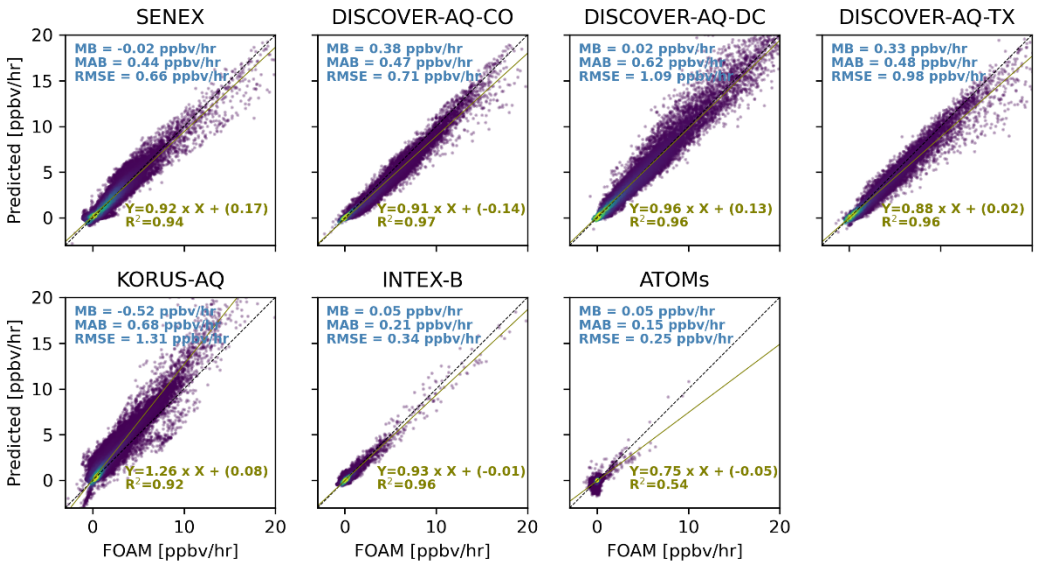

Figure S10. Each campaign dropped from training PO_3DNN and subsequently used as an independent benchmark.

Specific comments:

1. *Line 155: Unclear what the offset and slope mean.*

Response

Corrected.

Modifications

To correct for offset (additive bias) and slope (multiplicative bias) in this product

2. *Line 167: Why different cloud fraction thresholds are applied to NO2 vs. HCHO.*

Response

We strictly used the recommended values based on their user guide or commonly-used thresholds. However, it is important to note that, because PO3 is produced on daily basis from both HCHO and NO_2, a stricter flag between these products dictate where we should discard the unfit pixels. For instance, if ECF threshold is set to 10% for NO2, but 90% for HCHO, the 10% becomes the determining factor. As shown in this response letter, we don't think clouds will be a major problem in our analysis.

3. *Line 401: The assumption stated here seems questionable. MINDS-simulated water vapor and photolysis rates carry uncertainties, the influence of clouds and aerosols is not accounted for. These sources of uncertainty should be incorporated into the error analysis.*

Response

We addressed this in the reviewer's major comment.

It is not straightforward to characterize the errors in photolysis rates without precisely knowing 3D optical properties of clouds/aerosols and surface albedo reflectivity. While we could have thrown some numbers to propagate the errors, we think the quality of error characterization should be on par with the rest of the analysis.

4. *Figure 6: While the absolute PO3 values vary between bright and dim conditions, the spatial patterns (e.g., the ridgeline) appear consistent? It would be helpful to label the ridgeline across all panels.*

Response

While this is a valid point, we are against binarization of the atmospheric conditions. Having more red tapes on these contours will indirectly encourage people to see only the sign of the sensitivities, however, as stated in our work, we should consider the magnitude of the sensitivities to better describe ozone responses to its precursors.

5. *Figure 8: I'm having a hard time interpreting the sensitivity terms. What exactly do these sensitivities represent? Given that the magnitudes of photolysis rate, HCHO, and NO2 differ substantially, and that ozone chemistry is highly nonlinear, are these sensitivities additive?*

Response

We had provided the mathematical meaning of these sensitivities in Appendix A. They are the directional derivative providing the first-order sensitivity.

If we sum them, using a Taylor expansion, they will explain the first order approximation of PO3 minus a constant value. However, as the reviewer stated, PO3 is a non-linear problem and so is the DNN. So in order to better approximate PO3, we should also calculate higher order derivatives. We did not provide second-order sensitivities (which can be calculated in this way: $S^{(2)} = [C(+\Delta\epsilon) - 2C(0) + C(-\Delta\epsilon)]/(\Delta\epsilon)^2$ **), but we think the first-order sensitivities are adequate to describe the seasonality of PO3. Basically, the sum of these three terms explain most of the amplitude of the seasonality minus a constant offset.**

6. *Figure 8: The higher sensitivity of PO3 to HCHO in summer does not necessarily imply stronger sensitivity to VOC emissions. This may simply reflect the shared temperature dependence of PO3 and HCHO. In CTMs, ozone sensitivity is typically analyzed with respect to VOC emissions, whereas HCHO is an intermediate oxidation product rather than a primary species. The production of HCHO varies with VOC speciation, NOx levels and temperature.*

Response

This is a valid point, which is why we carefully specify that these sensitivities relate PO3 to HCHO and NO2 concentrations rather than emissions. The observed HCHO and NO2 concentrations reflect the integrated effects of emissions, meteorology, transport, deposition, and chemistry. Our approach captures these combined processes within the product, though we cannot separate their individual contributions.

Modifications

To reemphasize it we added:

Photolysis rates, which serve as crucial indicators of photochemical activity, are the primary determinants of PO_3 seasonality. Figure 8 illustrates the sensitivity of PO_3 to NO_2, HCHO, and

combined J-values (jNO_2 and jO^1D) based on Eq.3 across the same regions and months presented in Figure 7. The absolute values of PBL HCHO, NO_2, and jNO_2 are shown in Figure S3. As shown in Appendix A, these sensitivity values are influenced by both the magnitude of the precursor and the first derivative of PO_3 with respect to that precursor. Thus, the sensitivity values should be interpreted as the result of these combined effects. Moreover, these sensitivities are calculated with respect to local HCHO and NO_2 concentrations rather than local emissions (unlike typical modeling experiments). Local concentrations reflect the combined influence of both local and external emissions through various physicochemical processes.